

Comparison of Three Methods for the Derivation of a Biologic Scaffold Composed of Adipose Tissue Extracellular Matrix

Bryan N. Brown, Ph.D.,¹ John M. Freund, B.S.,¹ Li Han, Ph.D.,² J. Peter Rubin, M.D.,³ Janet E. Reing, M.S.,⁴
Eric M. Jeffries, B.S.,¹ Mathew T. Wolf, B.S.,¹ Stephen Tottey, Ph.D.,⁴ Christopher A. Barnes, Ph.D.,⁵
Buddy D. Ratner, Ph.D.,⁵ Stephen F. Badylak, D.V.M., M.D., Ph.D.⁴

Extracellular matrix (ECM)-based scaffold materials have been used successfully in both preclinical and clinical tissue engineering and regenerative medicine approaches to tissue reconstruction. Results of numerous studies have shown that ECM scaffolds are capable of supporting the growth and differentiation of multiple cell types *in vitro* and of acting as inductive templates for constructive tissue remodeling after implantation *in vivo*. Adipose tissue represents a potentially abundant source of ECM and may represent an ideal substrate for the growth and adipogenic differentiation of stem cells harvested from this tissue. Numerous studies have shown that the methods by which ECM scaffold materials are prepared have a dramatic effect upon both the biochemical and structural properties of the resultant ECM scaffold material as well as the ability of the material to support a positive tissue remodeling outcome after implantation. The objective of the present study was to characterize the adipose ECM material resulting from three methods of decellularization to determine the most effective method for the derivation of an adipose tissue ECM scaffold that was largely free of potentially immunogenic cellular content while retaining tissue-specific structural and functional components as well as the ability to support the growth and adipogenic differentiation of adipose-derived stem cells. The results show that each of the decellularization methods produced an adipose ECM scaffold that was distinct from both a structural and biochemical perspective, emphasizing the importance of the decellularization protocol used to produce adipose ECM scaffolds. Further, the results suggest that the adipose ECM scaffolds produced using the methods described herein are capable of supporting the maintenance and adipogenic differentiation of adipose-derived stem cells and may represent effective substrates for use in tissue engineering and regenerative medicine approaches to soft tissue reconstruction.

Introduction

THERE ARE A NUMBER OF surgical options for the repair of adipose tissue after trauma or resection. These options generally include the use of autologous tissue transplantation.^{1,2} Although these methods are generally sufficient for tissue repair, there are a number of limitations regarding the long-term survival and functionality of the transplanted tissue. These include both donor- and recipient-site morbidity, with many adipose tissue transplants experiencing volume reduction and necrosis due to disruption of the vascular supply.³ Methods that maintain the vascular sup-

ply during transplant are available. However, tissues transplanted using these methods are also subject to significant morbidity.³ A number of synthetic and biologically derived materials have been utilized as injectable tissue fillers and as volume filling constructs for soft tissue repair.^{4,5} However, these materials are often subject either to resorption and subsequent loss of volume and mechanical integrity or to a foreign body response that leads to an undesirable outcome due to chronic inflammation and encapsulation. Therefore, an off-the-shelf scaffold material that is capable of effectively supporting the growth, differentiation, and transplantation of adipose tissue-specific

¹Department of Bioengineering, McGowan Institute for Regenerative Medicine, University of Pittsburgh, Pittsburgh, Pennsylvania.

²Division of Plastic Surgery, Department of Surgery, University of Pittsburgh, Pittsburgh, Pennsylvania.

³Division of Plastic Surgery, Department of Surgery, McGowan Institute for Regenerative Medicine, University of Pittsburgh, Pittsburgh, Pennsylvania.

⁴McGowan Institute for Regenerative Medicine, University of Pittsburgh, Pittsburgh, Pennsylvania.

⁵Department of Chemical Engineering, University of Washington, Seattle, Washington.

cells without evoking a significant foreign body response is of great interest in the fields of plastic and reconstructive surgery.

The extracellular matrix (ECM) of each tissue and organ consists of the secreted products of its resident cell population. In turn, the phenotype and behavior of the resident cells is affected by signaling through the ECM, resulting in a state of dynamic reciprocity with the matrix.^{6–8} Thus, the ECM logically represents an appropriate substrate for the support of tissue-specific cell phenotype and function. Biologic scaffold materials composed of mammalian ECM have been harvested from a wide variety of tissues and organs, and recent work suggests that each of the ECM scaffold materials harvested from different tissues possesses a distinct composition and ultrastructure.⁹ However, it is unknown whether the tissue-specific composition and architecture of ECM scaffolds derived from individual organs are necessary to maintain the phenotype and three-dimensional arrangement of cells native to those same tissues compared with ECM materials derived from nonhomologous sources.^{10,11} Adipose tissue represents a potentially abundant source of ECM and may also represent an ideal scaffold material for the growth, differentiation, and phenotypic maintenance of cells that have been harvested from adipose tissue.^{12,13} However, the methods by which adipose tissue ECM scaffolds are produced may have distinct effects upon the structural and functional components of the resultant scaffold material and the subsequent ability of the material to function in *in vivo* tissue engineering and regenerative medicine applications.

In general, the methods used to decellularize and isolate ECM include a combination of physical (freezing, pressure, sonication, agitation) and chemical (enzyme, detergent, acid, alkaline) treatments that are typically tailored to the tissue or organ of interest.¹⁴ Logically, each of these treatments affects the components that are retained within the ECM and may alter the mechanical and material properties, ultrastructure, ability to support growth and differentiation of cells *in vitro*, and the host response after implantation.^{11,14–24} When tissues have been efficiently decellularized, the ECM-specific structural and functional components that remain (collagen, laminin, fibronectin, growth factors, etc.) are relatively well conserved across mammalian species and, therefore, do not evoke adverse immune reaction.^{25,26} However, a number of recent studies have shown that cellular components may remain after decellularization in a number of ECM materials, even those that have received approval for clinical use.²⁷ Further studies have suggested that inefficient removal of cellular contents such as DNA and the α -gal epitope during decellularization may be responsible for inflammation and poor outcomes after implantation.²⁸ However, when present in sufficiently small quantities, neither DNA nor the α -gal epitope has been associated with poor outcomes *in vivo*.^{29,30}

The objective of the present study was to characterize the adipose ECM material resulting from three distinct methods of decellularization—one method developed and optimized by the authors and two previously published methods—to determine the most effective method for the derivation of an adipose tissue ECM scaffold that was largely free of potentially immunogenic cellular content, including DNA and cytoplasmic lipid, while retaining adipose tissue-specific structural and functional components. The efficacy of removal of cellular content, the effect upon ultrastructure,

maintenance of several ECM components and growth factors, and the ability of the resulting material to support the *in vitro* growth and differentiation of adipose-derived stem cells (ADSCs) toward an adipogenic lineage were investigated for each method.

Materials and Methods

Preparation of adipose tissue ECM

Porcine adipose tissue was obtained from market weight pigs (~240–260 lbs.) at a local abattoir (Thoma's Meat Market, Saxonburg, PA). Tissue was frozen at -80°C before slicing into 3 mm sheets using a rotary blade. Adipose tissues were then treated with one of three decellularization methods as described below. Method A is an in-house method developed and optimized by the authors, and Methods B and C are methods previously described for the decellularization of adipose tissues.

Table 1 contains a summary of each decellularization method.

Method A. Method A was developed and optimized by the authors and represents a modification of a previously described method for decellularization of liver tissue.³¹ Both liver and adipose tissues represent solid organs with a three-dimensional structure that is not amenable to many mechanical methods of decellularization; therefore, the method relied primarily upon a set of chemical treatments that remove cellular content with minimal effects upon the three-dimensional ultrastructure of the remaining ECM.^{17,32} The reagents and times used in steps 1–13 (Table 1) of Method A were identical to those previously described for liver decellularization. However, after decellularization using the previously described protocol, it was found that large amounts of lipid remained within the tissues after completion of the protocol. Therefore, a series of experiments were performed in which the tissues were agitated in a variety of reagents in solution (water, ethanol, glycerol, corn oil, Triton-X 100, Triton-X 200, Tween 20, sodium dodecyl sulfate, deoxycholate, sodium hydroxide, isopropyl alcohol, and *n*-propanol) or agitated with dry reagents (Drierite, silica gel, sodium chloride, calcium chloride, talc, and alumina oxide). After each treatment the resultant tissues were examined and those methods that resulted in the greatest reduction of lipid were further investigated. The final steps of the protocol (i.e., steps 14–16) were chosen for their ability to remove residual lipid components and because of their simplicity and cost effectiveness.

Frozen adipose tissue was thawed in water and manually massaged to hasten the lysis of cells. Tissue was placed into a flask containing 0.02% trypsin–0.05% ethylenediaminetetraacetic acid (EDTA) solution, incubated at 37°C for 1 h, rinsed briefly in distilled deionized water (ddH₂O), and manually massaged again. Tissue was then placed into a flask containing 3% Triton X-100 and placed on an orbital shaker for 1 h at room temperature. After a brief water rinse, tissue was placed into a 4% deoxycholic acid solution and again placed on an orbital shaker for 1 h at room temperature. Tissue was rinsed three times in water and stored at 4°C overnight. The tissue was then subjected to a 4% ethanol and 0.1% peracetic acid solution on an orbital shaker for 2 h at room temperature followed by two phosphate-buffered sa-

TABLE 1. STEPS FOR EACH DECELLULARIZATION METHOD

Step #	Method A	Method B	Method C
1	Thaw tissue	Thaw tissue	Thaw tissue
2	Rinse in distilled deionized water	3 mg/g dry weight collagenase digestion	3 mg/g dry weight collagenase digestion
3	Mechanical massaging	0.02% trypsin/0.05% ethylenediaminetetraacetic acid	0.1% NP40
4	0.02% trypsin/0.05% ethylenediaminetetraacetic acid	10 U/mL deoxyribonuclease	4% sodium deoxycholate
5	Rinse in distilled deionized water	10 U/mL lipase	1% sodium dodecyl sulfate
6	Mechanical massaging	Rinse in PBS and distilled deionized water	0.9% NaCl in Tris-HCl w/protease inhibitors
7	3% triton X-100	Lyophilization	Rinse in PBS and distilled deionized water
8	Rinse in distilled deionized water		Lyophilization
9	4% sodium deoxycholate		
10	Rinse in distilled deionized water		
11	4% ethanol/0.1% peracetic acid		
12	Rinse in PBS and distilled deionized water		
13	Lyophilization		
14	100% n-propanol		
15	Rinse in distilled deionized water		
16	Lyophilization		

line (PBS, pH 7.4) and two water washes of 15 min each at room temperature. The resulting material was then washed in 100% n-propanol for 1 h on an orbital shaker at room temperature and washed in four changes of ddH₂O for 1 h to remove the n-propanol before lyophilization.

Method B. Frozen adipose tissue was thawed and then subjected to a previously described decellularization method.³³ Briefly, sheets of adipose tissue were subjected to collagenase digestion (3 mg/g starting tissue weight) for 1 h at 37°C on a shaker. The remaining tissue was then placed into a flask containing 0.02% trypsin–0.05% EDTA and 10 U/mL deoxyribonuclease in water for 1 h followed by 10 U/mL lipase for 1 h. The remaining material was then rinsed in PBS and then water three times each for 15 min per wash on an orbital shaker at room temperature and lyophilized.

Method C. Frozen adipose tissue was thawed and then subjected to a previously described decellularization method.³³ Briefly, sheets of adipose tissue were thawed and collagenase digestion (3 mg/g starting tissue weight) was performed for 1 h at 37°C on a shaker. The remaining tissue was then incubated in a flask containing 0.05% EDTA in water for 1 h followed by 0.1% nonyl phenoxy polyethylene alcohol (NP40) for 1 h, 4% sodium deoxycholate for 1 h, 1% sodium dodecyl sulfate for 1 h, and 0.9% NaCl in TRIS-HCl containing protease inhibitors (1 mM phenylmethylsulfonyl fluoride, 5 mM benzamide, and 10 mM N-ethylmaleimide) for 1 h on an orbital shaker at room temperature. The remaining material was then rinsed in PBS and water three times each for 15 min and lyophilized.

Characterization and confirmation of decellularization. Samples of materials resulting from each decellularization

method were fixed in formalin and embedded in paraffin or frozen in optimal cutting temperature solution then sectioned at 6 µm and affixed to glass slides. Oil red O staining was used to observe the lipid content remaining within each material. Decellularization of the scaffold materials was assessed by hematoxylin and eosin staining (H&E), immunofluorescent labeling with 4',6-diamidino-2-phenylindole (DAPI), quantification of the presence and length of any remaining DNA fragments by agarose gel electrophoresis, and quantification of DNA content by PicoGreen assay. All staining and assays were performed per manufacturer protocol or as previously described.²⁷ Materials were considered to be fully decellularized if no intact nuclei were visible in samples stained with H&E or sections labeled with DAPI, no DNA fragments with a length >200 bp were observed, and the total DNA content was <50 ng of double-stranded DNA/mg of scaffold dry weight. These values were selected based upon previous work that assessed levels of DNA remaining within commercially available ECM products.²⁷

Scanning electron microscopy

The ultrastructure of each sample was examined by scanning electron microscopy. Samples were fixed in cold 2.5% (v/v) glutaraldehyde in PBS for at least 24 h, followed by three washes in PBS. Lipid fixation was performed in 1% (w/v) osmium tetroxide (Electron Microscopy Sciences) for 1 h followed by three washes in PBS. Fixed samples were then dehydrated using a graded series of ethanol–water solutions (30%–100%) followed by 15 min in hexamethyldisilyzane and subsequent air-drying. The dried samples were mounted onto aluminum stubs and sputter coated with a 3.5 nm layer of gold–palladium alloy using a Sputter Coater 108 Auto (Cressington Scientific Instruments). Images were taken with a scanning electron microscope (JEOL JSM6330f)

at 1000× and 5000× magnification with an accelerating voltage of 3 kV.

Immunolabeling of ECM molecules

Formalin-fixed samples were embedded in paraffin for histologic sectioning. Samples were cut into 6 μm sections and affixed to glass slides. Before immunolabeling, the slides were dewaxed by immersion in xylenes followed by a graded series of ethanol-water solutions (100%–70%). Immunolabeling was performed with antibodies specific to a variety of ECM components (Table 2). Briefly, after dewaxing, all slides were subjected to antigen retrieval by immersion in 95°C–100°C in citric acid solution (10 mM, pH 6.0) followed by rinsing in a 1×Tris buffered saline/Tween-20 solution (0.1% Tween 20 v/v, pH 7.4). Samples were then washed in PBS and treated with a pepsin digestion (0.05% pepsin w/v in 10 mM HCl) solution for further antigen retrieval. Samples were blocked against nonspecific binding using a solution consisting of 2% serum, 1% bovine serum albumin, 0.1% Tween-20, and 0.1% Triton X-100 in PBS for 30 min at room temperature. Primary antibodies were diluted in the blocking solution (dilutions of all antibodies are listed in Table 2) and applied to sections overnight at 4°C. Samples were washed in PBS and appropriate fluorescently labeled secondary antibodies (AlexaFluor 488) were applied for 30 min at room temperature. All secondary antibodies were diluted 1:250 in the blocking solution. Slides were washed in PBS and coverslipped in the aqueous mounting medium before observation under a fluorescent microscope (Nikon e600).

Growth factor assay

Lyophilized samples were minced into pieces of ~3×3 mm. Six hundred milligrams of minced ECM were then suspended in 9 mL of urea-heparin extraction buffer (2 M urea and 5 mg/mL heparin in 50 mM tris with protease inhibitors: 1 mM phenylmethylsulfonyl fluoride, 5 mM benzamide, and 10 mM N-ethylmaleimide) at pH 7.4. The extraction mixture was rocked at 4°C for 20 to 24 h and then centrifuged at 3000 g for 30 min to separate remaining solid material from extracted supernatant. Supernatants were collected and 9 mL of freshly prepared urea-heparin extraction buffer was added to each pellet. Pellets with extraction buffer were re-extracted by rocking at 4°C for 20 to 24 h followed by centrifugation at 3000 g for 30 min, and supernatants were again collected. Supernatants from first and second extractions were dialyzed at 4°C against ddH₂O (total of three changes of dialysis water, 80–100 volumes per change) in Slide-A-Lyzer Dialysis Cassettes with a 3500

molecular weight cut off (Pierce Protein Research Products, Thermo-Fisher Scientific). The concentration of total protein in each extract was determined by the Bicinchoninic Acid Protein Assay (Pierce) following the manufacturer's protocol, and extracts were stored frozen in aliquots until time of assay.

Concentrations of basic fibroblast growth factor (bFGF) and vascular endothelial growth factor (VEGF) within urea-heparin extracts of adipose ECM samples were measured with the Quantikine Human bFGF Immunoassay (R&D Systems) and the Quantikine Human VEGF Immunoassay (R&D Systems). Concentrations of transforming growth factor beta 1 (TGF-β1) within urea-heparin extracts were measured with the Quantikine Mouse/Rat/Porcine/Canine TGF-β1 Immunoassay (R&D Systems). Manufacturer's instructions were followed for all three growth factor assays. Each assay for bFGF and VEGF was performed in duplicate; each assay for TGF-β1 was performed in triplicate. Each growth factor assay was performed two times. A one-way analysis of variance with Tukey's *post hoc* test was used to determine statistical significance.

Glycosaminoglycan assay

Glycosaminoglycan (GAG) concentrations were measured using the Blyscan Sulfated Glycosaminoglycan Assay Kit (Biocolor Ltd.). Samples were prepared by digestion of 50 mg/mL dry weight ECM in 0.1 mg/mL proteinase K in 10 mM Tris, pH 8.0, 50 mM NaCl, and 1 mM EDTA for 24 h at 50°C. Digested samples were then assayed following the manufacturer's protocol. Each assay was performed in duplicate. A one-way analysis of variance with Tukey's *post hoc* test was used to determine statistical significance.

ADSC culture on adipose ECM materials

Derivation of ADSCs. Human adipose tissue (obtained in accordance with IRB regulations) was digested in a collagenase solution (0.1% type 2 collagenase and 3.5% bovine serum albumin in 1× Hanks solution). After digestion of the adipose tissue, the resulting solution was filtered through gauze to remove undigested material. The filtered solution was then centrifuged at 10,000 rpm for 10 min at 20°C. Supernatant was removed and the pellet was resuspended in 10 mL of erythrocyte lysis buffer (154 mM NH₄Cl, 10 mM KHCO₃, and 1 mM EDTA in water, sterile filtered). Resuspended pellets were vortexed to lyse red blood cells and debris, and then recentrifuged at 10,000 rpm for 10 min at 20°C. The supernatant was then removed and the pellet resuspended in 10 mL of the ADSC culture medium (1:1 Dulbecco's modified Eagle Medium F-12, 10% fetal bovine serum, 0.1 mM penicillin, 0.06 mM streptomycin, 0.1 mM dexamethasone, and 10 mg/L gentamycin sulfate). Cells were expanded in culture for no more than 2 passages before being seeded onto ECM scaffolds.

ADSC viability on adipose ECM scaffolds. The ADSC culture medium was added to each adipose ECM and incubated in a 37°C, CO₂ regulated incubator for 24 h before cell seeding. 6×10⁵ ADSCs were seeded onto each of the adipose ECM materials and were maintained in the ADSC medium. Cell culture was stopped at 24 and 72 h postseeding and live/dead staining was performed.

TABLE 2. ANTIBODIES USED IN EXTRACELLULAR MATRIX IMMUNOLABELING

Antibody	Dilution	Company
Mouse anti-collagen I	1:2000	Sigma
Mouse anti-collagen III	1:2000	Sigma
Rabbit anti-collagen IV	1:200	Biodesign
Mouse anti-collagen VII	1:10	Abcam
Rabbit anti-laminin	1:200	Sigma

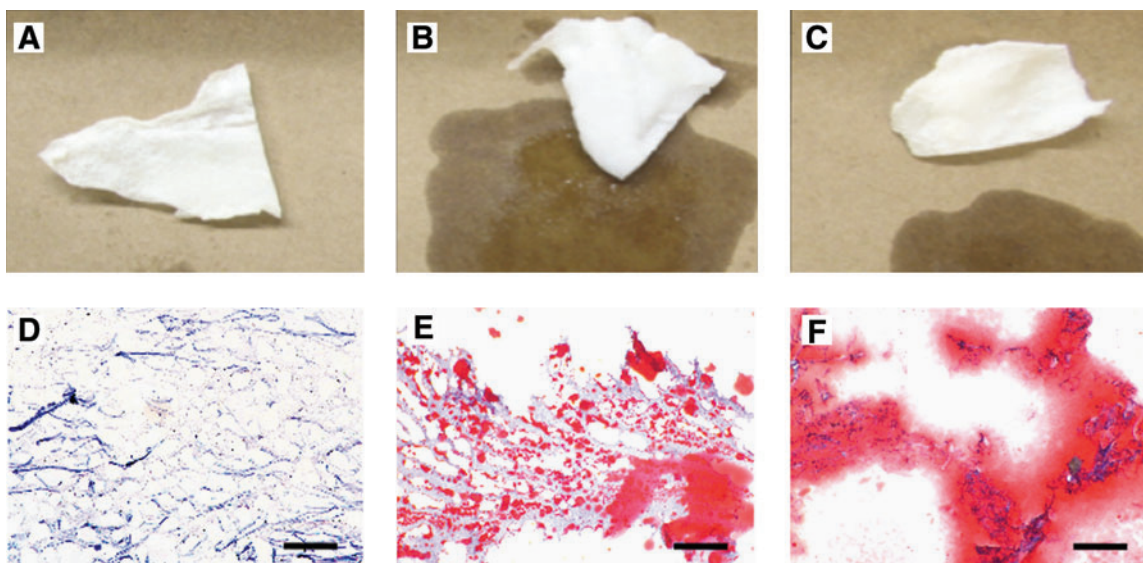


FIG. 1. Gross morphology (A–C) and oil red O staining (D–F, 10× magnification) of materials resulting from Method A (A, D), Method B (B, E), and Method C (C, F). Red staining is indicative of lipid content. Scale bar = 200 μm . Color images available online at www.liebertonline.com/tec.

For live/dead staining, the cell-seeded adipose ECM scaffolds were washed twice with PBS and then incubated for 10 min in a 1:1 mixture of 0.01 mg/mL (propidium-iodide [PI], Sigma Aldrich) and 5 $\mu\text{g}/\text{mL}$ (fluorescein diacetate [FDA], Sigma Aldrich). Seeded materials were then imaged using a confocal microscope (Olympus Fluoview 1000MP, Olympus America Inc.). Images were taken at sequential planes and flattened into one single plane using Metamorph software (Molecular Devices). Five different representative low power fields were taken from each sample and signal densities from PI and FDA measured with Metamorph software and used to determine the percentage of live and dead cells within the materials.

In vitro adipogenic differentiation of ADSCs on adipose ECM scaffolds. ADSCs (3×10^6) suspended in the ADSC culture medium were seeded onto the surface of each adipose ECM material and allowed to attach to the surface for 24 h. The ADSC medium was then replaced with the adipogenic medium (Zen-bio Inc.) for 7 days to induce differentiation of the ADSCs toward an adipogenic lineage followed by the adipogenic maintenance medium (Zen-bio Inc.) for another 7 days to test the ability of the ECM scaffold materials to support the maintenance of an adipogenic phenotype. After the 15 day culture period, the cell-seeded adipose ECM scaffolds were washed twice with PBS before staining with 1.5% v/v Adipo-Red (Lonza). Labeled samples

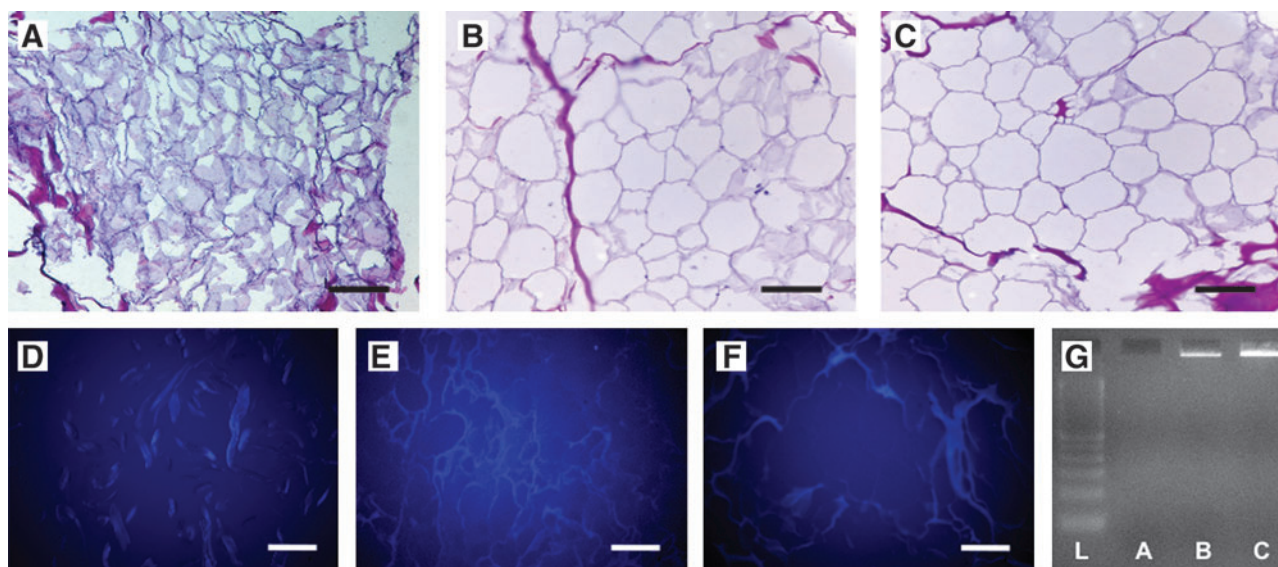


FIG. 2. Hematoxylin and eosin staining (A–C, 20× magnification), 4',6-diamidino-2-phenylindole labeling (D–F, 20× magnification), and results of agarose gel electrophoresis of DNA isolated from each scaffold type (G). Scale bar = 100 μm . Lane 1 = DNA ladder, lane 2 = Method A, lane 3 = Method B, lane 4 = Method C. Color images available online at www.liebertonline.com/tec.

were imaged using a confocal microscope (Olympus Fluoview 1000MP, Olympus America Inc.).

Results

Preparation of adipose tissue ECM

The adipose ECM produced using Method A yielded a dry, white, fibrous material, whereas Methods B and C both produced white materials with a wet, shiny surface appearance indicative of high lipid content (Fig. 1A–C). Staining with oil red O showed that there was little to no lipid in samples produced using Method A; however, lipid was shown to be present throughout samples produced using both Methods B and C (Fig. 1D–F). All materials were found to be durable and elastic during handling, while dry and also after rehydration. No intact nuclei were observed in tissue sections stained with H&E (Fig. 2A–C) or labeled with DAPI (Fig. 2D–F) for any of the three methods. Scaffolds produced using Method A did not appear to contain any DNA as shown by agarose gel electrophoresis (Fig. 2G). Scaffolds produced using Methods B and C were shown to contain DNA of high bp length as shown by gel electrophoresis (Fig. 2F). No DNA was detected by PicoGreen assay for scaffolds produced using Methods A and B. Scaffolds produced using Method C contained 78.1 ng DNA/mg scaffold dry weight.

Ultrastructural examination using scanning electron microscopy

Scanning electron micrographs were taken to examine the surface topography of the adipose ECM materials (Fig. 3). Both Methods B and C resulted in ECM with an uneven globular appearance at 1000 \times magnification indicative of high lipid content (Fig. 3B–C). Higher magnification (5000 \times , Fig. 3E–F) showed that these globules were smooth and

contiguous with the rest of the ECM surface. In contrast, Method A resulted in a rough and uneven surface architecture indicative of collagenous ECM components at all magnifications examined. (Fig. 3A, D) Smooth surfaces indicative of basement membrane and vascular structures were also visible throughout the scaffold material. Lipid droplets were observed in samples processed using Method A, but were less in size and number compared to those processed with Methods B and C. These results parallel those obtained using oil red O staining as described above.

Immunolabeling of ECM components

Immunolabeling showed that there were differences in the morphology and spatial distribution of a number of the ECM components investigated in this study, and that these differences were dependent on the decellularization protocol. Figure 4 shows immunolabeling of the scaffolds resulting from each decellularization protocol. Immunolabeling of native porcine adipose tissue is also shown. Positive labeling for collagen I was found within the fibrous connective tissue present between adipocyte lobules in all of the samples investigated; however, the ultrastructure of the collagen I fibers was disrupted by all of the decellularization methods investigated, resulting in a more loosely organized ultrastructure in the decellularized samples than was observed in the native tissue. Collagen III was found predominantly within the ECM surrounding adipocytes in native tissue and was also observed within the areas of fibrous connective tissue. Adipose tissue decellularized using Method A was positively labeled for collagen III primarily in the areas of the tissue formerly occupied by adipocytes, with similar results for tissues decellularized using Methods B and C. Collagen IV labeling was observed predominantly in the matrix associated with the adipocyte area and around blood vessels

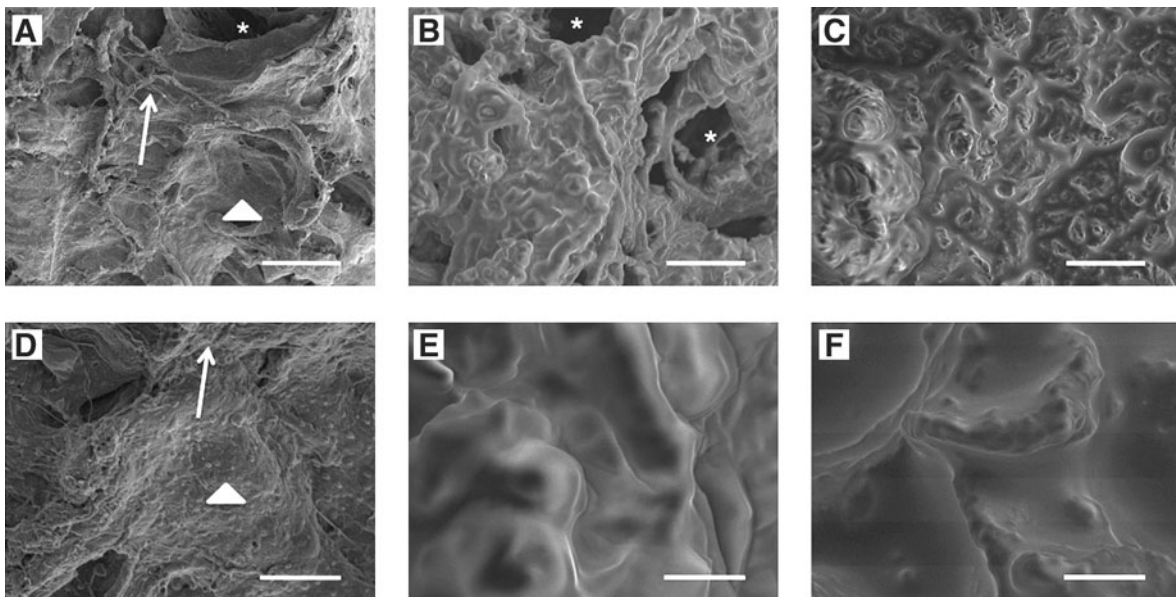


FIG. 3. Scanning electron micrographs of the surfaces of extracellular matrix (ECM) materials decellularized with Method A (A, D), Method B (B, E), and Method C (C, F). Top panel (A–C) = 1000 \times magnification, scale bar = 25 μ m. Bottom panel (D–F) = 5000 \times magnification, scale bar = 5 μ m. Asterisks indicate vascular structures. Arrows indicate exposed fibrous ECM structures. Arrowheads represent exposed smooth basement membrane like surfaces. Small lipid droplets can be observed in (A, D). Lipid surfaces indicated by smooth ultrastructure in (B, C, E, F) are contiguous across the surface of the material.

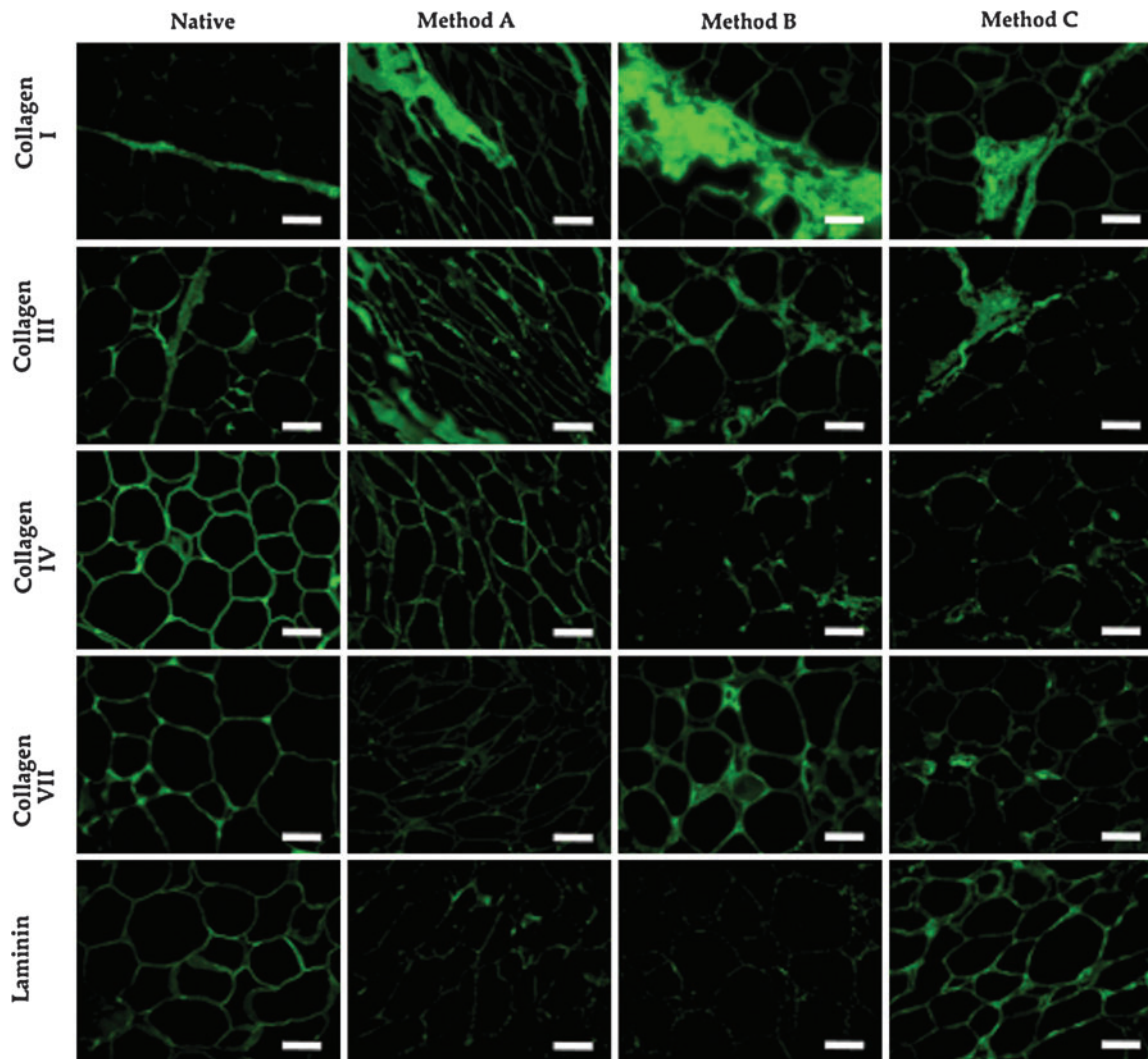


FIG. 4. Immunolabeling of collagen types I, III, IV, VII, and laminin in samples decellularized with Methods A, B, and C. Immunolabeling of native adipose tissue is shown for comparison. All images 20 \times magnification. Scale bar = 100 μ m. Color images available online at www.liebertonline.com/tec.

within native tissue. Positive labeling was observed in all decellularized samples. However, labeling for collagen type IV in samples decellularized using Method A had a morphology that more similar to that observed in native tissue than was observed in samples decellularized using Methods B or C. Small amounts of positive labeling for collagen VII were observed in the native adipose tissue. This labeling was located predominantly within the matrix present between adipocytes and near blood vessels. Only small areas of collagen VII labeling were observed in the decellularized tissues and labeling for collagen type VII in tissues decellularized using Methods B and C was found predominantly in the areas of remaining blood vessel structures, with little labeling observed in the matrix associated with former adipocytes. Minimal labeling for collagen type VII was observed in samples decellularized with Method A. Laminin was observed in the same areas as collagen type IV labeling. Laminin was largely removed by all decellularization processes; however, tissues decellularized using Method C showed labeling that was similar to that observed for native tissue.

Growth factor content

The three methods used to prepare adipose ECM resulted in differences in growth factor content within the resulting materials (Fig. 5). bFGF was present at a 1.4-fold higher concentration in adipose ECM prepared using Method A (2551.8 ± 148.1 pg/g dry weight) than in adipose ECM prepared using Method B (1840.5 ± 92.3 pg/g dry weight) ($p \leq 0.05$). 54.49 ± 6.39 pg/g dry weight of bFGF was detected in adipose ECM prepared using Method C. VEGF was present at low levels in adipose ECM prepared by Methods A and B (15.2 ± 13.0 pg/g dry weight and 27.6 ± 1.2 pg/g dry weight, respectively), but these values were not found to be significantly different. VEGF was not detected in adipose ECM prepared by Method C. TGF- β 1 was not detected in any of the porcine adipose ECM preparations.

GAG content

The three methods used to prepare adipose ECM resulted in differences in GAG content (Fig. 6). GAGs were present

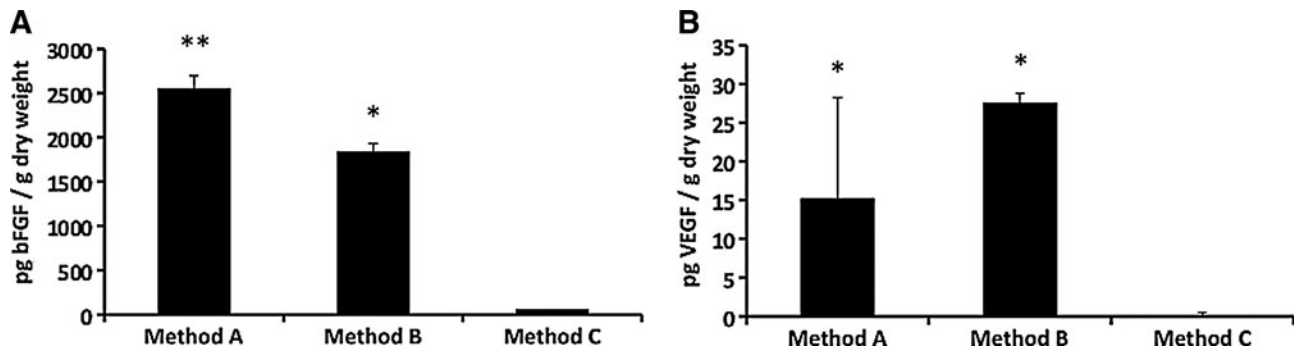


FIG. 5. Growth factor content of adipose ECM materials decellularized with Methods A, B, and C. Basic fibroblast growth factor (bFGF) content and vascular endothelial growth factor (VEGF) content are shown (A and B, respectively). Samples prepared using Methods A and B have higher bFGF and VEGF content than samples prepared with Method C ($p < 0.05$). Samples prepared using Method A have a higher bFGF content than samples prepared using Method B ($p < 0.05$). Results are shown as mean \pm standard error. **Method A samples have higher content than both Method B and Method C, $p < 0.05$. *Statistical significance compared to Method C, $p < 0.05$.

in ECM prepared using Methods A, B, and C at $1109.0 \pm 43.1 \mu\text{g/g}$ dry weight, $768.3 \pm 52.2 \mu\text{g/g}$ dry weight, and $95.2 \pm 4.3 \mu\text{g/g}$ dry weight, respectively. Adipose ECM prepared using method A had a 1.4-fold higher GAG content than the adipose ECM prepared using Method B ($p \leq 0.05$) and an 11.6-fold higher GAG content than porcine adipose ECM produced using Method C ($p \leq 0.05$). The GAG content of adipose ECM prepared by Method B was 8.1-fold higher than porcine adipose ECM prepared by Method C ($p \leq 0.05$).

ADSC culture

ADSCs were seeded onto adipose ECM scaffolds and cultured in the ADSC medium for 24 and 72 h and then subjected to the live/dead assay described above to check ADSC viability. As shown in Figure 7, approximately 95% of ADSCs seeded onto adipose ECM scaffolds and cultured in the ADSC culture medium were viable at 24 h after seeding and cell viability was approximately 99% at 72 h

postseeding regardless of preparation method. There were no significant differences in cell survival among the three different porcine adipose ECM used.

ADSCs were allowed to attach to the surface of each adipose ECM in the ADSC medium for 24 h before culture in the adipogenic medium for 7 days followed by the adipogenic maintenance medium for another 7 days. Cell-seeded scaffolds were then subjected to Adipo-Red labeling. As shown in Figure 8, ADSCs seeded onto the surface of the three different types of porcine adipose ECM and cultured in the adipocyte differentiation medium differentiated and maintained an adipocyte phenotype under *in vitro* conditions as evidenced by positive labeling using Adipo-Red, suggesting that all three types of porcine adipose ECM were able to support the *in vitro* growth and differentiation of ADSCs along an adipocyte lineage (Fig. 8).

Discussion

Adipose ECM materials resulting from three decellularization protocols were investigated for the effectiveness of re-

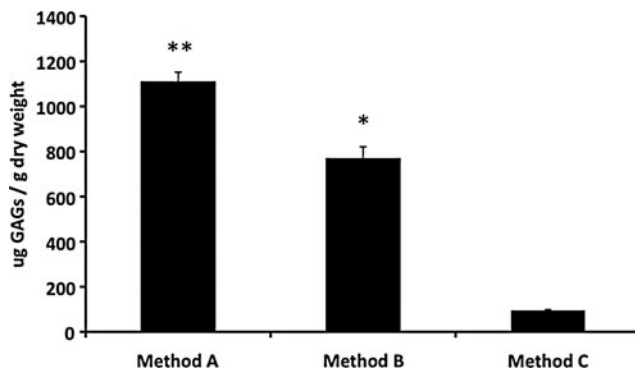


FIG. 6. Glycosaminoglycan (GAG) content of ECM scaffolds decellularized using Methods A, B, and C. GAG content of scaffolds decellularized with Method A are higher than in samples prepared using Methods B or C ($p < 0.05$), and levels in samples prepared with Method B are higher than in samples prepared using Method C. Results are shown as mean \pm standard error. **Method A samples have higher content than both Method B and Method C, $p < 0.05$. *Statistical significance compared to Method C, $p < 0.05$.

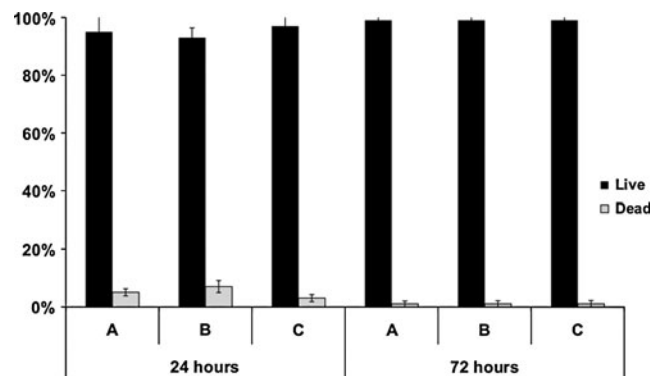


FIG. 7. Quantification of live/dead staining of adipose-derived stem cells seeded onto ECM scaffolds decellularized using Methods A, B, and C at 24 and 72 h postseeding. No significant differences in cell viability were observed for any of the scaffold materials investigated. Percent live cells is represented by black bars. Percent dead cells is represented by white bars. Results are shown as mean \pm standard error.

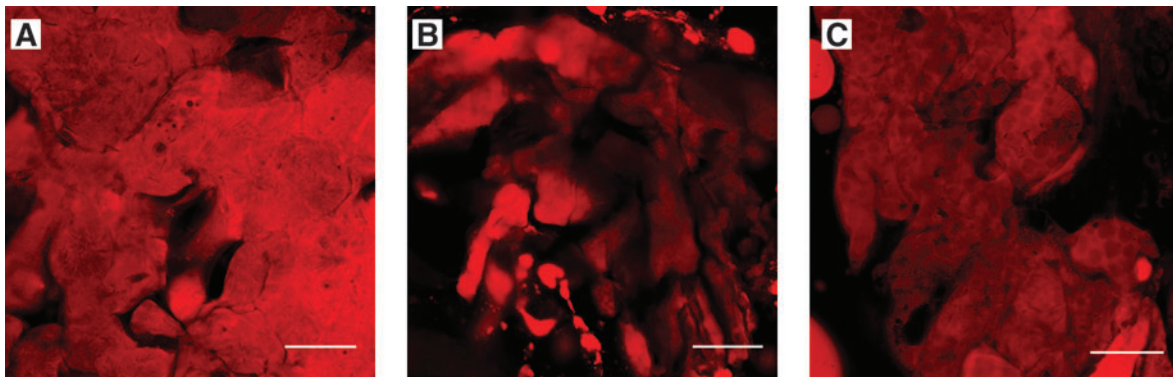


FIG. 8. Adipo-Red labeling of adipose-derived stem cells seeded onto ECM scaffolds decellularized using Methods A, B, and C, respectively. Scale bar = 50 μm . Color images available online at www.liebertonline.com/tec.

removal of cellular content, ultrastructure, ECM component molecule content and distribution, and the ability to support the growth and adipogenic differentiation of ADSCs. Results show that each of the three decellularization methods investigated resulted in set of scaffold characteristics that was distinct from both a structural and biochemical perspective. Although these findings are not surprising given the differences in the decellularization agents used in each method, the results of the present study demonstrate the importance of determining a decellularization protocol that is tailored to the tissue of interest; that is, a process that removes as much of the cellular material as possible with minimal adverse effects upon the biochemical composition, topographical ligand landscape, and biologic activity of the resulting scaffold material.¹⁴

In the present study, Method A was shown to produce a scaffold material that had a surface topography that more closely resembled the fibrous and basement membrane ECM components of adipose tissue than did Method B or C, which possessed a topography that was indicative primarily of lipid structures at the surface of the scaffold material. Further examination of these materials using oil red O staining showed that Method A retained little to no lipid content after decellularization, whereas scaffolds processed using Methods B or C retained lipid content. Examination of the materials using immunolabeling showed that each decellularization method was associated with maintenance of a distinct set of ECM component molecules within the resultant scaffold. The spatial organization of these components was similar to that observed in native adipose tissue, suggesting that all of the decellularization processes maintained the structure of the native tissue to a large degree. Biochemical analysis showed that Method A retained more of the GAG and bFGF content than did Method B or C. Both Methods A and B were more efficient in maintenance of overall GAG and growth factor content than was Method C, which resulted in significantly lower quantities of both GAG and growth factors within the resulting scaffold material. Despite the differences in structure and biochemical content observed in the present study, no differences were seen in the ability of the materials to support the *in vitro* growth, differentiation, and maintenance of ADSCs along an adipocyte lineage. However, the lack of differences in *in vitro* growth characteristics may have resulted from similarities in the adsorption of proteins from the cell culture medium to each of the ECM materials. The ability of ADSCs to differ-

entiate toward lineages other than adipogenic was not investigated in the current study.

Recent evidence suggests that tissue-specific ECM may be more effective in supporting the maintenance of highly specific cell phenotypes. For example, a recent study showed that ECM scaffolds derived from the liver were more effective in supporting the maintenance of the phenotype of hepatic sinusoidal endothelial cells during *in vitro* culture than were ECM scaffolds composed of urinary bladder or small intestinal submucosa.¹¹ The ability of certain ECM scaffolds to promote the maintenance of specific phenotypes and differentiation states may be related to differences in tissue-specific architecture and molecular composition that have been observed in a number of recent studies; however, it is unclear whether the structural or the functional components of the material play a larger role in determining the outcome of cell-scaffold interactions.^{9,17,18}

Many studies have shown that ECM scaffolds are capable of supporting the growth of a variety of cell types *in vitro* as well as acting as templates for the functional reconstruction of a wide variety of tissues and organs *in vivo*. Although the mechanisms by which these materials support and promote a constructive remodeling process are only partially understood, it appears clear that rapid degradation of the scaffold material with concurrent release of both intact growth factors and newly generated bioactive matricryptic peptides as well as the provision of unique surface architectures are factors that play an important role.³⁴⁻⁴¹ The ability to promote constructive remodeling *in vivo* has also been shown to be highly dependent on the methods used in preparing the scaffold material.^{19,20,42} For example, chemical crosslinking is often used to increase the mechanical strength of a scaffold material, to slow degradation, or to mask cellular epitope that may remain within the scaffold material after decellularization. Although the rationale for using crosslinking in the production of ECM scaffold materials is understood, a number of studies that have compared noncrosslinked matrices to matrices that have been crosslinked using chemical methods have shown a less desirable tissue remodeling response when ECM scaffolds have been altered using chemical crosslinking.^{20,42,43} The exact reasons for the differences in tissue remodeling are not clear, but are likely related to the inability of the material to degrade and release bioactive components or through alteration of the bioactive ligands present on the surface of the scaffold material.

Similarly, a recent study showed that the presence of a large amount of cellular content within an ECM scaffold led to a more inflammatory type host response after implantation and resulted in the formation of scar tissue within the site of remodeling.⁴⁴ This response is in contrast to the constructive remodeling that was observed when the same material was effectively decellularized before implantation, again highlighting the importance of the methods of production in determining the tissue remodeling outcome associated with implantation of an ECM scaffold material.

The results of this study showed that Methods A and B resulted in efficient decellularization of adipose tissue, whereas Method C did not (78.1 ng DNA/mg dry weight). Although the scaffolds resulting from each decellularization method examined in this study supported the growth and differentiation of ADSCs, there is concern that incomplete decellularization may lead to an adverse host response after implantation, which will affect the downstream ability of the scaffold material to support constructive remodeling *in vivo*. Further, the effects of the excess cytoplasmic lipid observed within the biologic scaffolds produced using Methods B and C upon *in vivo* remodeling are unknown, but indicate that potentially immunogenic cellular contents may remain within the scaffold materials. Furthermore, the presence of excess lipid may adversely affect the ability to process these scaffold materials into a configuration that is applicable for clinical approaches to tissue reconstruction.

Conclusion

Three methods for the preparation of decellularized adipose tissue were compared for effectiveness of decellularization, ability to maintain the structure and functional composition of ECM components, and the ability to support the growth and adipogenic differentiation of ADSCs. The results of the study showed that each decellularization method was associated with distinct structure and composition of the resulting material. Despite these differences, the ability to support the growth and adipogenic differentiation of ADSCs was unaffected. However, only Methods A and B achieved effective decellularization of the adipose tissue, and only Method A was shown to remove the majority of the lipid content of the adipose tissue. The presence of cellular remnants, including excess lipid, may affect the ability of an adipose ECM material to function as a template for constructive remodeling *in vivo*. This study shows the importance of the decellularization protocol and suggests that adipose ECM scaffolds derived using Method A as described herein may represent an effective substrate for use in tissue engineering and regenerative medicine approaches to soft tissue reconstruction.

Acknowledgments

This work was supported by NIH grants R01 AR054940 (SFB), R01 CA114246 (JPR), and EB-002027 (NESAC/BIO—University of Washington). Bryan Brown was supported by NIH fellowship F31 EB007914.

Disclosure Statement

No competing financial interests exist.

References

1. Tachi, M., and Yamada, A. Choice of flaps for breast reconstruction. *Int J Clin Oncol* **10**, 289, 2005.
2. Butterwick, K.J., Nootheti, P.K., Hsu, J.W., and Goldman, M.P. Autologous fat transfer: an in-depth look at varying concepts and techniques. *Facial Plast Surg Clin North Am* **15**, 99, viii, 2007.
3. Wu, L.C., Bajaj, A., Chang, D.W., and Chevray, P.M. Comparison of donor-site morbidity of SIEA, DIEP, and muscle-sparing TRAM flaps for breast reconstruction. *Plast Reconstr Surg* **122**, 702, 2008.
4. Patrick, C.W., Jr. Tissue engineering strategies for adipose tissue repair. *Anat Rec* **263**, 361, 2001.
5. Choi, J.H., Gimble, J.M., Lee, K., Marra, K.G., Rubin, J.P., Yoo, J.J., *et al.* Adipose tissue engineering for soft tissue regeneration. *Tissue Eng Part B Rev* **16**, 413, 2010.
6. Bissell, M.J., Hall, H.G., and Parry, G. How does the extracellular matrix direct gene expression? *J Theor Biol* **99**, 31, 1982.
7. Boudreau, N., Myers, C., and Bissell, M.J. From laminin to lamin: regulation of tissue-specific gene expression by the ECM. *Trends Cell Biol* **5**, 1, 1995.
8. Ingber, D. Extracellular matrix and cell shape: potential control points for inhibition of angiogenesis. *J Cell Biochem* **47**, 236, 1991.
9. Badylak, S.F., Freytes, D.O., and Gilbert, T.W. Extracellular matrix as a biological scaffold material: structure and function. *Acta Biomater* **5**, 1, 2009.
10. Sellaro, T.L., Ranade, A., Faulk, D.M., McCabe, G.P., Dorko, K., Badylak, S.F., *et al.* Maintenance of human hepatocyte function *in vitro* by liver-derived extracellular matrix gels. *Tissue Eng Part A* **16**, 1075, 2010.
11. Sellaro, T.L., Ravindra, A.K., Stolz, D.B., and Badylak, S.F. Maintenance of hepatic sinusoidal endothelial cell phenotype *in vitro* using organ-specific extracellular matrix scaffolds. *Tissue Eng* **13**, 2301, 2007.
12. Flynn, L.E. The use of decellularized adipose tissue to provide an inductive microenvironment for the adipogenic differentiation of human adipose-derived stem cells. *Biomaterials* **31**, 4715, 2010.
13. Choi, J.S., Yang, H.J., Kim, B.S., Kim, J.D., Lee, S.H., Lee, E.K., *et al.* Fabrication of porous extracellular matrix scaffolds from human adipose tissue. *Tissue Eng Part C Methods* **16**, 387, 2010.
14. Gilbert, T.W., Sellaro, T.L., and Badylak, S.F. Decellularization of tissues and organs. *Biomaterials* **27**, 3675, 2006.
15. Liao, J., Joyce, E.M., and Sacks, M.S. Effects of decellularization on the mechanical and structural properties of the porcine aortic valve leaflet. *Biomaterials* **29**, 1065, 2008.
16. Badylak, S.F., Valentin, J.E., Ravindra, A.K., McCabe, G.P., and Stewart-Akers, A.M. Macrophage phenotype as a determinant of biologic scaffold remodeling. *Tissue Eng* **14**, 1835, 2008.
17. Brown, B., Lindberg, K., Reing, J., Stolz, D.B., and Badylak, S.F. The basement membrane component of biologic scaffolds derived from extracellular matrix. *Tissue Eng* **12**, 519, 2006.
18. Brown, B.N., Barnes, C.A., Kasick, R.T., Michel, R., Gilbert, T.W., Beer-Stolz, D., *et al.* Surface characterization of extracellular matrix scaffolds. *Biomaterials* **31**, 428, 2010.
19. Brown, B.N., Valentin, J.E., Stewart-Akers, A.M., McCabe, G.P., and Badylak, S.F. Macrophage phenotype and remodeling outcomes in response to biologic scaffolds with and without a cellular component. *Biomaterials* **30**, 1482, 2009.
20. Valentin, J.E., Badylak, J.S., McCabe, G.P., and Badylak, S.F. Extracellular matrix bioscaffolds for orthopaedic applications.

- A comparative histologic study. *J Bone Joint Surg Am* **88**, 2673, 2006.
21. Williams, C., Liao, J., Joyce, E.M., Wang, B., Leach, J.B., Sacks, M.S., *et al.* Altered structural and mechanical properties in decellularized rabbit carotid arteries. *Acta Biomater* **5**, 993, 2009.
 22. Gratzner, P.F., Harrison, R.D., and Woods, T. Matrix alteration and not residual sodium dodecyl sulfate cytotoxicity affects the cellular repopulation of a decellularized matrix. *Tissue Eng* **12**, 2975, 2006.
 23. Harrison, R.D., and Gratzner, P.F. Effect of extraction protocols and epidermal growth factor on the cellular repopulation of decellularized anterior cruciate ligament allografts. *J Biomed Mater Res A* **75**, 841, 2005.
 24. Rieder, E., Kasimir, M.T., Silberhumer, G., Seebacher, G., Wolner, E., Simon, P., *et al.* Decellularization protocols of porcine heart valves differ importantly in efficiency of cell removal and susceptibility of the matrix to recellularization with human vascular cells. *J Thorac Cardiovasc Surg* **127**, 399, 2004.
 25. Allman, A.J., McPherson, T.B., Badylak, S.F., Merrill, L.C., Kallakury, B., Sheehan, C., *et al.* Xenogeneic extracellular matrix grafts elicit a TH2-restricted immune response. *Transplantation* **71**, 1631, 2001.
 26. van der Rest, M., and Garrone, R. Collagen family of proteins. *FASEB J* **5**, 2814, 1991.
 27. Gilbert, T.W., Freund, J.M., and Badylak, S.F. Quantification of DNA in biologic scaffold materials. *J Surg Res* **152**, 135, 2009.
 28. Zheng, M.H., Chen, J., Kirilak, Y., Willers, C., Xu, J., and Wood, D. Porcine small intestine submucosa (SIS) is not an acellular collagenous matrix and contains porcine DNA: possible implications in human implantation. *J Biomed Mater Res B Appl Biomater* **73**, 61, 2005.
 29. Raeder, R.H., Badylak, S.F., Sheehan, C., Kallakury, B., and Metzger, D.W. Natural anti-galactose alpha1,3 galactose antibodies delay, but do not prevent the acceptance of extracellular matrix xenografts. *Transpl Immunol* **10**, 15, 2002.
 30. Daly, K.A., Stewart-Akers, A.M., Hara, H., Ezzelarab, M., Long, C., Cordero, K., *et al.* Effect of the alphaGal epitope on the response to small intestinal submucosa extracellular matrix in a nonhuman primate model. *Tissue Eng Part A* **15**, 3877, 2009.
 31. Lin, P., Chan, W.C., Badylak, S.F., and Bhatia, S.N. Assessing porcine liver-derived biomatrix for hepatic tissue engineering. *Tissue Eng* **10**, 1046, 2004.
 32. Brown, B.N., Barnes, C.A., Kasick, R.T., Michel, R., Gilbert, T.W., Beer-Stolz, D., *et al.* Surface characterization of extracellular matrix scaffolds. *Biomaterials* **31**, 428, 2010.
 33. Katz, A.J., Llull, R., Futrell, W.J., Hedrick, M.H., Benhaim, P., Lorenz, H.P., *et al.* Adipose-derived stem cells and lattices, U.S. Patent #6777231, 2004.
 34. Beattie, A.J., Gilbert, T.W., Guyot, J.P., Yates, A.J., and Badylak, S.F. Chemoattraction of progenitor cells by remodeling extracellular matrix scaffolds. *Tissue Eng Part A* **15**, 1119, 2009.
 35. Brennan, E.P., Reing, J., Chew, D., Myers-Irvin, J.M., Young, E.J., and Badylak, S.F. Antibacterial activity within degradation products of biological scaffolds composed of extracellular matrix. *Tissue Eng* **12**, 2949, 2006.
 36. Brennan, E.P., Tang, X.H., Stewart-Akers, A.M., Gudas, L.J., and Badylak, S.F. Chemoattractant activity of degradation products of fetal and adult skin extracellular matrix for keratinocyte progenitor cells. *J Tissue Eng Regen Med* **2**, 491, 2008.
 37. Chun, S.Y., Lim, G.J., Kwon, T.G., Kwak, E.K., Kim, B.W., Atala, A., *et al.* Identification and characterization of bioactive factors in bladder submucosa matrix. *Biomaterials* **28**, 4251, 2007.
 38. Haviv, F., Bradley, M.F., Kalvin, D.M., Schneider, A.J., Davidson, D.J., Majest, S.M., *et al.* Thrombospondin-1 mimetic peptide inhibitors of angiogenesis and tumor growth: design, synthesis, and optimization of pharmacokinetics and biological activities. *J Med Chem* **48**, 2838, 2005.
 39. Li, F., Li, W., Johnson, S., Ingram, D., Yoder, M., and Badylak, S. Low-molecular-weight peptides derived from extracellular matrix as chemoattractants for primary endothelial cells. *Endothelium* **11**, 199, 2004.
 40. Reing, J.E., Zhang, L., Myers-Irvin, J., Cordero, K.E., Freytes, D.O., Heber-Katz, E., *et al.* Degradation products of extracellular matrix affect cell migration and proliferation. *Tissue Eng Part A* **15**, 605, 2009.
 41. Sarikaya, A., Record, R., Wu, C.C., Tullius, B., Badylak, S., and Ladisch, M. Antimicrobial activity associated with extracellular matrices. *Tissue Eng* **8**, 63, 2002.
 42. Badylak, S.F., Valentin, J.E., Ravindra, A.K., McCabe, G.P., and Stewart-Akers, A.M. Macrophage phenotype as a determinant of biologic scaffold remodeling. *Tissue Eng Part A* **14**, 1835, 2008.
 43. Valentin, J.E., Turner, N.J., Gilbert, T.W., and Badylak, S.F. Functional skeletal muscle formation with a biologic scaffold. *Biomaterials* **31**, 7475, 2010.
 44. Brown, B.N., Valentin, J.E., Stewart-Akers, A.M., McCabe, G.P., and Badylak, S.F. Macrophage phenotype and remodeling outcomes in response to biologic scaffolds with and without a cellular component. *Biomaterials* **30**, 1482, 2009.

Address correspondence to:

Stephen Badylak, D.V.M., M.D., Ph.D.

McGowan Institute for Regenerative Medicine

University of Pittsburgh

Suite 300

450 Technology Drive

Pittsburgh, PA 15219

E-mail: badylaks@upmc.edu

Received: June 09, 2010

Accepted: November 02, 2010

Online Publication Date: February 2, 2011

